Research Article Vol. 30, No. 4 / 14 Feb 2022 / Optics Express 6388
Optics EXPRESS

Deterministic distribution of multipartite entanglement in a quantum network by continuous-variable polarization states

LIANG WU,[1,2,3] TING CHAI,[1] YANHONG LIU,[4] YAOYAO ZHOU,[4] JILIANG QIN,[2,5] ZHIHUI YAN,[2,5,*] AND XIAOJUN JIA[1,2,5]

[1]College of Physics and Electronic Engineering, Shanxi University, 92 Wucheng Road, Taiyuan 030006, China
[2]State Key Laboratory of Quantum Optics and Quantum Optics Devices, Institute of Opto-Electronics, Shanxi University, 92 Wucheng Road, Taiyuan 030006, China
[3]College of Information Engineering, Shanxi Vocational University of Engineering Science and Technology, 369 Wenhua Street, Jinzhong 030619, China
[4]Department of Physics, Taiyuan Normal University, 319 University Street, Jinzhong 030619, China
[5]Collaborative Innovation Center of Extreme Optics, Shanxi University, 92 Wucheng Road, Taiyuan 030006, China
*zhyan@sxu.edu.cn

Abstract: Quantum network plays a vitally important role in the practical application of quantum information, which requires the deterministic entanglement distribution among multiple remote users. Here, we propose a feasible scheme to deterministically distribute quadripartite entanglement by continuous-variable (CV) polarization states. The quantum server prepares the quadripartite CV polarization entanglement and distributes them to four remote users via optical fiber. In this way, the measurement of CV polarization entanglement is local oscillation free, which makes the long distance entanglement distribution in commercial optical fiber communication networks possible. Furthermore, both the Greenberger-Horne-Zeilinger-like (GHZ-like) and cluster-like polarization entangled states can be distributed among four users by controlling the beam splitter network in quantum server, which are confirmed by the extended criteria for polarization entanglement of multipartite optical modes. The protocol provides the direct reference for experimental implementation and can be directly extended to quantum network with more users, which is essential for a metropolitan quantum network.

1. Introduction

Quantum entanglement is the central concept of quantum mechanics, and exhibits the unpredictable prospect in quantum communication [1,2], quantum computation [3] and quantum metrology [4–6]. Light has the advantages of the fast transmission speed and weak interaction with the environment, which is the ideal carrier for quantum information [7–10]. The use of the optical quantum entanglement at the telecommunication wavelength offers the possibility to implement the quantum communication protocols, such as quantum key distribution [11], quantum teleportation [12,13] and quantum secret sharing [14]. The distribution of optical entangled states over a long distance is not only of interest in the understanding of physical mechanism such as decoherence, and but also of crucial importance in the application of a quantum network [8,15–17]. So far, great progress has been demonstrated in discrete variable entanglement distribution via the fiber and free-space quantum channels [18,19], continuous-variable (CV) quantum information paves an alternative approach, and information is encoded in the position or momentum quadrature of optical modes due to the advantages of deterministic generation, manipulation and measurement [20,21]. Thus the deterministic distribution of bipartite entanglement over 20 km has been experimentally realized [22]. With the development of quantum information, quantum network,

#451062 https://doi.org/10.1364/OE.451062
Journal © 2022 Received 14 Dec 2021; revised 1 Feb 2022; accepted 1 Feb 2022; published 11 Feb 2022

Optics EXPRESS

which can implement quantum information tasks among multiple remote users, is demanding for practical applications [23–27].

Quantum network consists of quantum server and quantum users. The CV quantum information has the advantages of high efficiency generation, manipulation and detection [28,29]. Several generation theories of multipartite quadrature entanglement have been proposed [30,31]. However, the distribution of quadrature entanglement is difficult, because the complicated measurement of quadrature requires a strong local optical field. In addition, the quantum optical field that can directly interact with quantum node is required for quantum network. The bipartite polarization entanglement at the fiber transmission window has been generated by coupling the polarization squeezed light field generated by the optical fiber Sagnac effect, which is suitable for quantum communication [32,33]. With the development of quantum network, the deterministic distribution of multipartite entanglement is demanded, and the distribution of multipartite CV polarization state can overcome these problems in metropolitan quantum networks consisting of commercial fiber channels. Differentiating the multipartite quadrature entanglement, there is another kind of quantum correlation of Stokes parameters on Poincare sphere among multipartite CV polarization entangled optical modes, which corresponds to the Stokes parameters on Bloch sphere of atoms, and thus enable to directly interact with atomic nodes [34]. Besides, the measurement of multipartite CV polarization entanglement of optical modes is local oscillation free, which can overcome the phase fluctuation in fibers and thus is suitable for long distance transmission [35–38].

In the work of Ref. [30], the research is only focused on the generation principle of GHZ-like and cluster-like quadripartite quadrature entanglement. In this work, however, we propose an experimentally feasible scheme to deterministically distribute multipartite entanglement by means of CV polarization states instead of quadrature states. Our scheme is implemented by transferring the quadripartite quadrature entanglement to CV polarization entanglement, and then distributing them through the commercial optical fiber channels, which overcomes the phase fluctuation during the fiber transmission for long-distance quantum distribution. Based on the quadripartite inseparability criteria of Stokes operators for GHZ-like and cluster-like states, the two kinds of distributed entanglement are verified. Moreover, the long distance distributions of two different kinds of GHZ-like and cluster-like CV polarization entanglement can be realized by controlling the special beam splitter status, which can be applied in controlled quantum teleportation network [39], the quantum secret sharing network [14], and one-way quantum computation [40]. Furthermore, the scheme of the CV polarization entanglement distribution is scalable. Since the CV quadrature entanglements with much more optical modes have been prepared experimentally [3,41], the presented scheme can be directly extended to distribute CV polarization entangled states with more optical modes. Thus, our scheme provides the direct reference for experiment implementation and is the valuable and scalable quantum resource for practical applications.

2. Generation and distribution of CV GHZ-like and cluster-like quadripartite entanglement

Figure 1 provides a schematic for the generation and distribution of quadripartite entangled states. In quantum server, four quadrature squeezed states of light are generated from two NOPAs and transformed into the spatially separated polarization entangled states of optical fields. GHZ-like and cluster-like states can be obtained by controlling the interference phase of the beam splitter, respectively.

The quadrature amplitude and phase operators of the optical field can be expressed by the annihilation operator $\hat{a}$ and creation operator $\hat{a}^\dagger$ as: $\hat{X}_i = \frac{1}{2}(\hat{a}^\dagger + \hat{a})$, $\hat{Y}_i = -\frac{1}{2}i(\hat{a}^\dagger - \hat{a})$. When the light field is coherent state or vacuum state, the quantum fluctuation variance are $V(\hat{X}) = V(\hat{Y}) = \frac{1}{4}$. The NOPA consists of a type II crystal and an optical cavity. When the NOPA1 and NOPA2

Optics EXPRESS

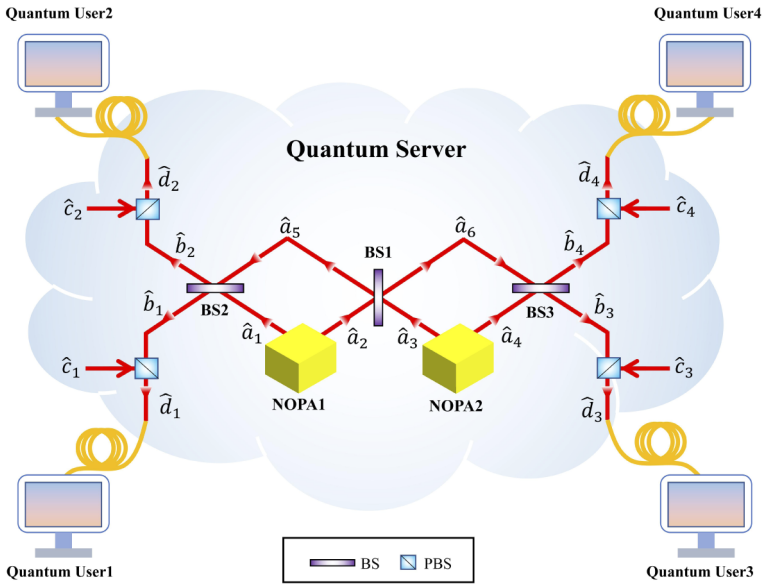

Fig. 1. The schematic of CV GHZ-like and cluster-like quadripartite polarization entangled optical fields using two NOPAs and beam splitter network. BS_{1-3}: beam splitter. PBS: polarization beam splitter. Yellow squares: NOPAs. Dark yellow curve: communication optical fiber. The entangled state light field is distributed to four users.

run in the parameter de-amplification state, two quadrature phase squeezed state of optical fields $(\hat{a}_1, \hat{a}_4)$ and two quadrature amplitude squeezed state of optical fields $(\hat{a}_2, \hat{a}_3)$ can be generated. Beams $\hat{a}_{1-4}$ interfere on the beam splitter system. For quadrature entanglement, $\theta_{(i=1,2,3)}$ represents the relative phase between injected optical modes on BSi (i=1,2,3). The phase difference θ_1 between $\hat{a}_2$ and $\hat{a}_3$ on the BS1 is controlled to $(\frac{1}{2}+k)\pi$ (k is an integer), the phase difference $\theta_{2(3)}$ on the BS2(3) are all controlled to $2k\pi$ to generate a quadripartite GHZ-like quadrature entangled state. However, if the phase difference θ_3 between $\hat{a}_4$ and $\hat{a}_6$ on the BS3 is controlled to $(\frac{1}{2}+k)\pi$, a cluster-like quadripartite quadrature entangled state can be produced.

The output fields $\hat{a}_5$ and $\hat{a}_6$ can be expressed as:

$$\begin{aligned}\hat{a}_5 &= \frac{1}{\sqrt{2}}\left(\hat{a}_2 + \hat{a}_3 e^{i\theta_1}\right)\\ \hat{a}_6 &= \frac{1}{\sqrt{2}}\left(\hat{a}_2 - \hat{a}_3 e^{i\theta_1}\right)\end{aligned} \tag{1}$$

A GHZ-like or cluster-like quadripartite quadrature entangled states would be obtained by the above method.

$$\begin{aligned}\hat{b}_1 &= \frac{1}{\sqrt{2}}\left(\hat{a}_1 + \hat{a}_5 e^{i\theta_2}\right)\\ \hat{b}_2 &= \frac{1}{\sqrt{2}}\left(\hat{a}_1 - \hat{a}_5 e^{i\theta_2}\right)\\ \hat{b}_3 &= \frac{1}{\sqrt{2}}\left(\hat{a}_6 + \hat{a}_4 e^{i\theta_3}\right)\\ \hat{b}_4 &= \frac{1}{\sqrt{2}}\left(\hat{a}_6 - \hat{a}_4 e^{i\theta_3}\right)\end{aligned} \tag{2}$$

Optics EXPRESS

In quantum mechanics, Stokes operators $\hat{S}_0$, $\hat{S}_1$, $\hat{S}_2$, $\hat{S}_3$ are usually used to describe the polarization state of light, $\hat{S}_0$ represents the beam intensity, whereas $\hat{S}_1$, $\hat{S}_2$, $\hat{S}_3$ characterize its polarization and form a Cartesian axes system, which can be easily mapped to the spin operators of the atomic media. The Stokes operators can be expressed by means of the creation operator $\hat{a}^{\dagger}_{H(V)}$ and annihilation operator $\hat{a}_{H(V)}$ of horizontal and vertical polarization mode: $\hat{S}_0 = \hat{a}^{\dagger}_H\hat{a}_H + \hat{a}^{\dagger}_V\hat{a}_V, \hat{S}_1 = \hat{a}^{\dagger}_H\hat{a}_H - \hat{a}^{\dagger}_V\hat{a}_V, \hat{S}_2 = \hat{a}^{\dagger}_H\hat{a}_V e^{i\varphi} + \hat{a}^{\dagger}_V\hat{a}_H e^{-i\varphi}, \hat{S}_3 = i\hat{a}^{\dagger}_V\hat{a}_H e^{-i\varphi} - i\hat{a}^{\dagger}_H\hat{a}_V e^{i\varphi}$. In the definition of Stokes operators, φ is used to express the relative phase between the H and V polarization modes.

From the commutation relation of generation and annihilation operators: $[\hat{a}_k, \hat{a}_j] = \delta_{k,j}(k,j \in \{H, V\})$, the quantum fluctuations of the Stoke operator can be written as [37]:

$$\begin{aligned} V_0 = V_1 &= a_V^2\delta^2\hat{X}_V + a_H^2\delta^2\hat{X}_H, \\ V_2(\varphi) = V_3(\varphi + \frac{\pi}{2}) &= \cos^2\varphi(a_V^2\delta^2\hat{X}_H + a_H^2\delta^2\hat{X}_V) + \sin^2\varphi(a_V^2\delta^2\hat{Y}_H + a_H^2\delta^2\hat{Y}_V), \end{aligned} \tag{3}$$

where $\hat{X}_{V(H)}$, $\hat{Y}_{V(H)}$ is the quadrature amplitudes (phases) fluctuation of $V(H)$ polarized light. Their mean values and variances satisfy the following Heisenberg uncertainty relationships: $V_1V_2 \geq |\langle\hat{S}_3\rangle|, V_2V_3 \geq |\langle\hat{S}_1\rangle|, V_1V_3 \geq |\langle\hat{S}_2\rangle|$.

According to the definition of Stokes operator, the polarization entangled states $\hat{d}$ could be obtained by coupling horizontally (vertically) polarized quadrature entangled states $\hat{b}$ with vertically (horizontally) polarized strongly coherent light field $\hat{c}$ on a polarization beam splitter (PBS). The power of coherent light is much larger than quadrature entangled states of light ($\alpha_c \gg \alpha_b$), and the phase difference φ between the vertical and horizontal direction is $\frac{\pi}{2}$, so a polarization entangled state light field can be obtained.

3. Distribution of CV GHZ-like and cluster-like quadripartite polarization entanglement

The resulting polarization entangled states are transmitted in the fibers. The relationship between transmission efficiency and transmission distance is: $t = 10^{-\frac{\zeta l}{10}}$, where t is the transmission efficiency of optical fiber, ζ is the transmission loss, and l is the transmission distance. A typical transmission losses of 0.2 dB/km at 1550 nm in optical fiber is employed in our scheme to quantify the two kinds of polarization entangled states transmission distance. When the polarization entangled state light field propagates in the optical fiber, the Stokes operators quantum fluctuation variances of quadripartite polarization entangled states can be expressed as:

$$\begin{aligned} \delta^2\left(\hat{S}_{2d_i}\right) &= \frac{\alpha_C^2}{4}\left[t\left(\eta\xi_2\xi_3 e^{2r_2} + \eta\xi_2\xi_3 e^{-2r_3} + 2\eta\xi_1 e^{-2r_1} - 2\eta\xi_2\xi_3 - 2\eta\xi_1\right) + 4\right] \\ \delta^2\left(\hat{S}_{2d_j}\right) &= \frac{\alpha_c^2}{4}\left[t\left(\eta\xi_2\xi_3 e^{2r_2} + \eta\xi_2\xi_3 e^{-2r_3} + 2\eta\xi_4 e^{\mp 2r_4} - 2\eta\xi_2\xi_3 - 2\eta\xi_4\right) + 4\right] \\ \delta^2\left(\hat{S}_{3d_i}\right) &= \frac{\alpha_c^2}{4}\left[t\left(\eta\xi_2\xi_3 e^{-2r_2} + \eta\xi_2\xi_3 e^{2r_3} + 2\eta\xi_1 e^{2r_1} - 2\eta\xi_2\xi_3 - 2\eta\xi_1\right) + 4\right] \\ \delta^2\left(\hat{S}_{3d_j}\right) &= \frac{\alpha_c^2}{4}\left[t\left(\eta\xi_2\xi_3 e^{-2r_2} + \eta\xi_2\xi_3 e^{2r_3} + 2\eta\xi_4 e^{\pm 2r_4} - 2\eta\xi_2\xi_3 - 2\eta\xi_4\right) + 4\right] \end{aligned} \tag{4}$$

here, r_{1-4} are the squeezing factors for $\hat{a}_{1-4}$, which depends on the strength and duration of the parametric interaction in NOPA, the transmission losses in optical device are unavoidable, and ξ_2 represents the optical transmission efficiency in quantum server of from NOPA1(2) to BS1, while ξ_3 is that for from BS1 to BS2(3), $\xi_{1(4)}$ means that for from NOPA1(2) to BS2(3), respectively. And η is the detection efficiency. For symbols $\pm$ and $\mp$ represent the GHZ-like state and cluster-like state, respectively. Where $\delta^2(\hat{S}_{2d_{i(j)}})$ and $\delta^2(\hat{S}_{3d_{i(j)}})$ $(i,j = 1,2,3,4)$ are the variances of Stokes operators of beam $\hat{d}_{1-4}$.

Optics EXPRESS

The inseparability criterion is a sufficient condition for entanglement. Duan, van Loock and Furusawa proposed the bipartite and multipartite inseparability criterion for quadrature respectively [31,42], and Lam's group extend the bipartite quadrature entangled states inseparability criteria to bipartite polarization entangled states [35]. In 2015, the tripartite inseparability criterion of Stokes operators for optical beams was deduced [43]. According to the definition and commutation relation of Stokes operators, we can obtain the GHZ-like quadripartite inseparability criterion of Stokes operators for optical beams $\hat{d}^G_{1-4}$, which is characterized by the combination of correlation variances I^G_m $(m = 1, 2, 3, 4)$:

$$\begin{aligned}
I^G_1 &\equiv \frac{\delta^2(\hat{S}_{2_{d^G_2}} - \hat{S}_{2_{d^G_3}}) + \delta^2(g_1\hat{S}_{3_{d^G_1}} + \hat{S}_{3_{d^G_2}} + \hat{S}_{3_{d^G_3}} + g_4\hat{S}_{3_{d^G_4}})}{4\left|\alpha_c^2 - \alpha_a^2\right|} \geq 1,\\
I^G_2 &\equiv \frac{\delta^2(\hat{S}_{2_{d^G_1}} - \hat{S}_{2_{d^G_4}}) + \delta^2(\hat{S}_{3_{d^G_1}} + g_2\hat{S}_{3_{d^G_2}} + g_3\hat{S}_{3_{d^G_3}} + \hat{S}_{3_{d^G_4}})}{4\left|\alpha_c^2 - \alpha_a^2\right|} \geq 1,\\
I^G_3 &\equiv \frac{\delta^2(\hat{S}_{2_{d^G_1}} - \hat{S}_{2_{d^G_2}}) + \delta^2(\hat{S}_{3_{d^G_1}} + \hat{S}_{3_{d^G_2}} + g_3\hat{S}_{3_{d^G_3}} + g_4\hat{S}_{3_{d^G_4}})}{4\left|\alpha_c^2 - \alpha_a^2\right|} \geq 1,\\
I^G_4 &\equiv \frac{\delta^2(\hat{S}_{2_{d^G_3}} - \hat{S}_{2_{d^G_4}}) + \delta^2(g_1\hat{S}_{3_{d^G_1}} + g_2\hat{S}_{3_{d^G_2}} + \hat{S}_{3_{d^G_3}} + \hat{S}_{3_{d^G_4}})}{4\left|\alpha_c^2 - \alpha_a^2\right|} \geq 1,
\end{aligned} \tag{5}$$

where d^G_{1-4} represents the four GHZ-like optical modes, and g_i $(i = 1, 2, 3, 4)$ is the gain factor. If any three of the above inequalities are violated simultaneously, the four optical modes are CV GHZ-like quadripartite polarization entangled states.

In the same way, we can get the quadripartite criterion of the cluster-like state Stocks operators, which is characterized by the combination of correlation variances I^C_m $(m = 5, 6, 7)$:

$$\begin{aligned}
I^C_5 &\equiv \frac{\delta^2(\hat{S}_{2_{d^C_1}} - \hat{S}_{2_{d^C_2}}) + \delta^2(\hat{S}_{3_{d^C_1}} + \hat{S}_{3_{d^C_2}} + g_7\hat{S}_{3_{d^C_3}})}{4\left|\alpha_c^2 - \alpha_a^2\right|} \geq 1,\\
I^C_6 &\equiv \frac{\delta^2(\hat{S}_{3_{d^C_3}} - \hat{S}_{3_{d^C_4}}) + \delta^2(-g_6\hat{S}_{2_{d^C_2}} + \hat{S}_{2_{d^C_3}} + \hat{S}_{2_{d^C_4}})}{4\left|\alpha_c^2 - \alpha_a^2\right|} \geq 1,\\
I^C_7 &\equiv \frac{\delta^2(g_5\hat{S}_{3_{d^C_1}} + \hat{S}_{3_{d^C_2}} + 2\hat{S}_{3_{d^C_3}}) + \delta^2(-2\hat{S}_{2_{d^C_2}} + \hat{S}_{2_{d^C_3}} + g_8\hat{S}_{2_{d^C_4}})}{4\left|\alpha_c^2 - \alpha_a^2\right|} \geq 2,
\end{aligned} \tag{6}$$

where d^C_{1-4} represents the four cluster-like optical modes, and g_i $(i = 5, 6, 7, 8)$ is the gain factor. If the above inequalities are violated simultaneously, the CV quadripartite cluster-like polarization entangled states would be verified.

Since NOPAs and the detection systems are working in the same states, we assume that $g_i = g$ $(i = 1, 2, 3, 4)$ and $r_{1-4} = r$ to simplify the calculation process. Thus, for GHZ-like state, the combinations of correlation variances $I_1 = I_2$, $I_3 = I_4$; and $I_5 = I_6$ for cluster-like state. The expressions of the optimal gains (g_{opt}) for I_{1-4} can be obtained by calculating the minimum values of the Eq. (5), as:

$$\begin{aligned}
g^G_{opt_1} &= \frac{\eta(\xi_1 + \xi_4)e^{4r} + \eta e^{2r}(2\xi_2\xi_3 - \xi_1 - \xi_4) - 2\eta\xi_2\xi_3}{\eta\xi_4(\xi_1 + \xi_4)e^{4r} + e^{2r}(4 - 2\eta\xi_2\xi_3 - \eta\xi_1 - \eta\xi_4) + 2\eta\xi_2\xi_3},\\
g^G_{opt_2} &= \frac{(e^{4r} - 1)\eta\xi_2\xi_3}{2e^{2r}(1 - \eta\xi_2\xi_3) + \eta\xi_2\xi_3(e^{4r} + 1)}.
\end{aligned} \tag{7}$$

For cluster-like state, the expressions of g_6, g_7 are basically the same, expect the difference between ξ_1 and ξ_4. For simplicity, we make $\xi_1 = \xi_4 = \xi$. Similarly for g_5 and g_8. By calculating

Optics EXPRESS

the minimum value of equations (6), the dependence of the g_{opt} on the squeezing parameters can be obtained as follows:

$$\begin{aligned} g^{C}_{opt_{6(7)}} &= \frac{2\eta\xi_2\xi_3(e^{4r}-1)}{4e^{2r}+2\eta\xi(1-e^{2r})+\eta\xi_2\xi_3(e^{2r}-1)^2}, \\ g^{C}_{opt_{5(8)}} &= \frac{2\eta\xi(e^{4r}-e^{2r})-4\eta\xi_2\xi_3+\eta\xi_2\xi_3(e^{2r}+1)^2}{4e^{2r}+2\eta\xi(e^{4r}-e^{2r})+\eta\xi_2\xi_3(e^{2r}-1)^2}. \end{aligned} \tag{8}$$

Here, we choose a relatively easy to be obtained experimental value $r = 1.27$, which means the squeezing degree of the light is 11 dB, to characterize the dependency relationship between the correlation variances I_m $(m = 1-7)$ and distribution distance L. Figure 2 show the dependence of the combination of correlation variances I_m $(m = 1-7)$ on the distribution distance L in optical fiber. The trace (i) corresponding normalized shot noise limited (SNL), while traces (ii), (iii) and (iv) are for I_{1-4}, $I_{5,6}$ and I_7, respectively. The main factors limiting the distribution distance are the squeezing parameters r, optical transmission efficiency ξ_{1-4} in quantum server, fiber transmission efficiency t, and the detection efficiency η . When both the detection efficiency η and the transmission efficiencies ξ_{1-4} are equal to 0.98, the distribution distance of GHZ-like polarization entangled state can reach 5.17 km, and the maximum distribution distance of cluster-like state is 4.89 km. If the squeezing parameters r, optical transmission efficiency ξ_{1-4} in quantum server, fiber transmission efficiency t, and the detection efficiency η are optimized, the maximum distribution distance can be improved.

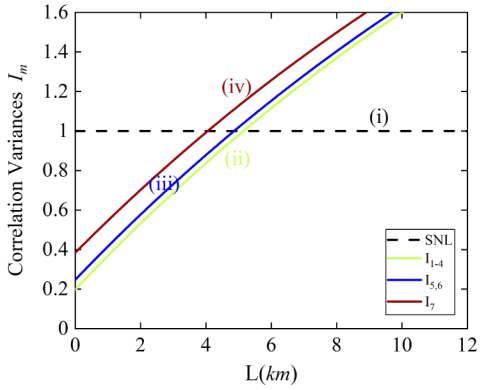

Fig. 2. Normalized curves of the combination of correlation variances I_m versus distribution distance L with the squeezing factor $r = 1.27$, $g_i = g_{opt}$ and $\eta = \xi_{1-4} = 0.98$. Traces (i), (ii), (iii) and (iv) are for SNL, I_{1-4}, $I_{5,6}$ and I_7, respectively.

Figure 3 shows the dependence of the combination of correlation variances I_m $(m = 1-7)$ on the squeezing factor r with different distribution distances $L = 0$ km, 2 km, 4 km, respectively. Trace (i) is the corresponding SNL, dash and solid lines with different colour of traces (ii), (iii) and (iv) in subgraphs (a), (c) are the theoretical fitting curve correspond to the curves of $I_{1-4,7}$ with $g = 1$ and $g = g_{opt}$ as $\eta = \xi_{1-4} = 0.98$, respectively. Similarly, the dash lines and solid lines (ii), (iii) and (iv) in subgraphs (b) are the theoretical fitting curve correspond to $I_{5,6}$ with $g = 2$ and $g = g_{opt}$.

Table 1 shows the dependence of minimum requirement of squeezing parameter r on distribution distance L. When the value of distribution distance and gain factor are given, the minimum requirement of squeezing parameter r means when squeezing parameter is larger than this minimum required value r, the inseparability criteria for CV polarization states can be violated and the distributions of multipartite entanglements can be realized. Some cases are shown

Optics EXPRESS

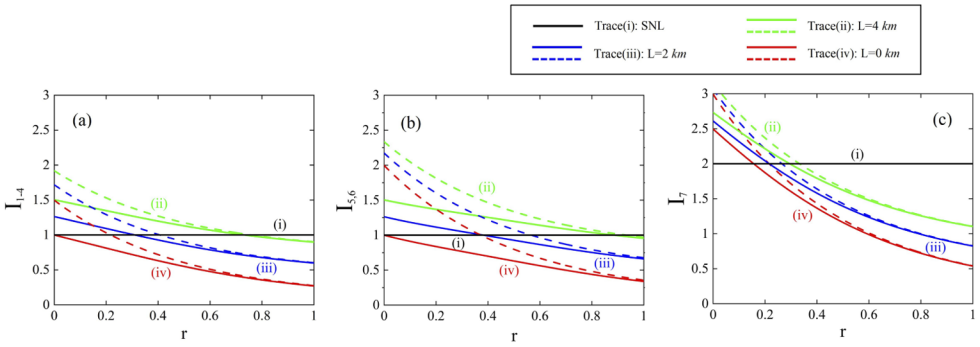

Fig. 3. Normalized curves of the combination of correlation variances I_m versus squeezing factor r with different distribution distances when $L = 4\ km$, $L = 2\ km$, $L = 0\ km$. Subgraph (a) is for GHZ-like States, subgraph (b) and (c) are for cluster-like States. Trace (i) is the SNL, trace (ii)-(iv) with different colour are the correlation variances I_{1-7} for different distribution distances. Dash(solid) line in subgraph (a) and (c) means $g = 1(g_{opt})$, while in subgraph (b) means $g = 2(g_{opt})$.

as follow: when $g = 1$ and r is larger than 0.217, 0.407, 0.76, respectively, the distribution distances can be greater than 0 km, 2 km, 4 km for GHZ-like states. When optimized gain factor is taken, the minimum required squeezing factor r is larger than 0, 0.311 and 0.733, respectively, which correspond to the distribution distances greater than 0 km, 2 km and 4 km, respectively. The optimization gain factor can effectively loose the requirement of squeezing factor. For the cluster-like state with the optimized gain factors, squeezing factor r is larger than 0, 0.383 and 0.885, the inseparability criteria I_5 and I_6 with the transmission distances greater than 0 km, 2 km and 4 km can be violated. When squeezing factor of r is larger than 0.157, 0.217 and 0.296, the inseparability criterion I_7 with the transmission distances greater than 0 km, 2 km and 4 km can be violated. Thus, the minimum requirement of squeezing factor of r is larger than 0.157, 0.383 and 0.885, which guarantee the successful distribution of cluster state.

Table 1. Dependence of Minimum Requirement of Squeezing Parameter r on Distribution Distance L.

Distribution Distance	GHZ-Like		Cluster-Like			
$L\ (km)$	I_{1-4}		$I_{5,6}$		I_7	
	$g = 1$	$g = g_{opt}$	$g = 2$	$g = g_{opt}$	$g = 1$	$g = g_{opt}$
0	r>0.217	r>0	r>0.373	r>0	r>0.217	r>0.157
2	r>0.407	r>0.311	r>0.566	r>0.383	r>0.266	r>0.217
4	r>0.760	r>0.733	r>0.932	r>0.885	r>0.334	r>0.296

4. Conclusions

In summary, we propose a scheme to deterministically distribute quantum entanglement among four remote users in a network by polarization states. In a quantum network, a quantum server prepares CV polarization entangled states, and distributes entanglement to multiple remote users among whom quantum correlation is shared. Moreover, two kinds of quadripartite CV polarization entanglement can be distributed by controlling the experimental parameters in the beam splitter network. Additionally, this scheme can be combined with existing commercial fiber telecommunication networks directly. The CV quadrature entanglement with much more submodes has been prepared experimentally [41], the presented method can be directly extended

Optics EXPRESS

to prepare polarization entangled states with more submodes and distribute quantum resources for more remote users, which could take a step forward in studying potential applications in a quantum communication network.

Funding. National Natural Science Foundation of China (11904218, 62135008, 61775127, 11947133, 12004276, 11804246); National Outstanding Youth Foundation of China (62122044); China National Funds for Distinguished Young Scientists (61925503); Program for Sanjin Scholars of Shanxi Province; Program for the Outstanding Innovative Teams of Higher Learning Institutions of Shanxi; Natural Science Foundation of Shanxi Province(201801D221009); Scientific and Technological Innovation Programs of Higher Education Institutions in Shanxi (2019L0092,2020L0029); Fund for Shanxi Key Subjects Construction, "1131" Project Key Subjects.

Disclosures. The authors declare no conflicts of interest.

Data availability. Data underlying the results presented in this paper are not publicly available at this time but may be obtained from the authors upon reasonable request.

References

1. W. Zhang, D. Ding, Y. Sheng, L. Zhou, B. Shi, and G. Guo, "Quantum secure direct communication with quantum memory," Phys. Rev. Lett. **118**(22), 220501 (2017).
2. G. He, J. Zhu, and G. Zeng, "Quantum secure communication using continuous variable Einstein-Podolsky-Rosen correlations," Phys. Rev. A **73**(1), 012314 (2006).
3. X. Su, S. Hao, X. Deng, L. Ma, M. Wang, X. Jia, C. Xie, and K. Peng, "Gate sequence for continuous variable one-way quantum computation," Nat. Commun. **4**(1), 2828 (2013).
4. G. Tóth and L. Apellaniz, "Quantum metrology from a quantum information science perspective," J. Phys. A: Math. Theor. **47**(42), 424006 (2014).
5. X. Zuo, Z. Yan, Y. Feng, J. Ma, X. Jia, C. Xie, and K. Peng, "Quantum interferometer combining squeezing and parametric amplification," Phys. Rev. Lett. **124**(17), 173602 (2020).
6. F. Hudelist, J. Kong, C. Liu, J. Jing, Z. Ou, and W. Zhang, "Quantum metrology with parametric amplifier-based photon correlation interferometers," Nat. Commun. **5**(1), 3049 (2014).
7. H. Zhong, H. Wang, Y. Deng, M. Chen, L. Peng, Y. Luo, J. Qin, D. Wu, X. Ding, Y. Hu, P. Hu, X. Yang, W. Zhang, H. Li, Y. Li, X. Jiang, L. Gan, G. Yang, L. You, Z. Wang, L. Li, N. Liu, C. Lu, and J. Pan, "Quantum computational advantage using photons," Science **370**(6523), 1460–1463 (2020).
8. H. J. Kimble, "The quantum internet," Nature **453**(7198), 1023–1030 (2008).
9. C. Okoth, A. Cavanna, T. Santiago-Cruz, and M. Chekhova, "Microscale generation of entangled photons without momentum conservation," Phys. Rev. Lett. **123**(26), 263602 (2019).
10. G. Frascella, S. Agne, F. Y. Khalili, and M. V. Chekhova, "Overcoming detection loss and noise in squeezing-based optical sensing," NPJ Quantum Inf. **7**(1), 72 (2021).
11. L. S. Madsen, V. C. Usenko, M. Lassen, R. Filip, and U. L. Andersen, "Continuous variable quantum key distribution with modulated entangled states," Nat. Commun. **3**(1), 1083 (2012).
12. A. Furusawa, J. Sorensen, S. Braunstein, C. A. Fuchs, H. J. Kimble, and E. S. Polzik, "Unconditional quantum teleportation," Science **282**(5389), 706–709 (1998).
13. M. Huo, J. Qin, Z. Yan, Z. Qin, X. Su, X. Jia, C. Xie, and K. Peng, "Deterministic quantum teleportation through fiber channels," Sci. Adv. **4**(10), 9401 (2018).
14. Y. Zhou, J. Yu, Z. Yan, X. Jia, J. Zhang, C. Xie, and K. Peng, "Quantum secret sharing among four players using multipartite bound entanglement of an ptical field," Phys. Rev. Lett. **121**(15), 150502 (2018).
15. J. Pan, Z. Chen, C. Lu, H. Weinfurter, A. Zeilinger, and M. Zukowski, "Multiphoton entanglement and interferometry," Rev. Mod. Phys. **84**(2), 777–838 (2012).
16. C. Chou, J. Laurat, H. Deng, K. Choi, H. de Riedmatten, D. Felinto, and H. J. Kimble, "Functional quantum nodes for entanglement distribution over scalable quantum networks," Science **316**(5829), 1316–1320 (2007).
17. X. Jia, Z. Yan, Z. Duan, X. Su, H. Wang, C. Xie, and K. Peng, "Experimental realization of three color entanglement at optical fiber communication and atomic storage wavelength," Phys. Rev. Lett. **109**(25), 253604 (2012).
18. J. Ren, P. Xu, H. Yong, L. Zhang, S. Liao, J. Yin, W. Liu, W. Cai, M. Yang, L. Li, K. Yang, X. Han, Y. Yao, J. Li, H. Wu, S. Wan, L. Liu, D. Liu, Y. Kuang, Z. He, P. Shang, C. Guo, R. Zheng, K. Tian, Z. Zhu, N. Liu, C. Lu, R. Shu, Y. Chen, C. Peng, J. Wang, and J. Pan, "Ground-to-satallite quantum teleportation," Nature **549**(7670), 70–73 (2017).
19. I. Marcikic, H. de Riedmatten, W. Tittel, H. Zbinden, and N. Gisin, "Long-distance teleportation of qubits at telecommunication wavelengths," Nature **421**(6922), 509–513 (2003).
20. C. Weedbrook, S. Pirandola, R. Garcia-Patron, N. J. Cerf, T. Ralph, J. H. Shapiro, and S. Lloyd, "Gaussian quantum information," Rev. Mod. Phys. **84**(2), 621–669 (2012).
21. S. L. Braunstein and P. van Loock, "Quantum information with continuous variables," Rev. Mod. Phys. **77**(2), 513–577 (2005).
22. J. Feng, Z. Wan, Y. Li, and K. Zhang, "Distribution of continuous variable quantum entanglement at a telecommunication wavelength over 20km of optical fiber," Opt. Lett. **42**(17), 3399–3402 (2017).
23. S. Liu, Y. Lou, and J. Jing, "Orbital angular momentum multiplexed deterministic all-optical quantum teleportation," Nat. Commun. **11**(1), 3875 (2020).

Optics EXPRESS

24. W. Wang, K. Zhang, and J. Jing, "Large-scale quantum network over 66 orbital angular momentum optical modes," Phys. Rev. Lett. **125**(14), 140501 (2020).
25. S. Li, X. Pan, Y. Ren, H. Liu, S. Yu, and J. Jing, "Deterministic generation of orbital-angular-momentum multiplexed tripartite entanglement," Phys. Rev. Lett. **124**(8), 083605 (2020).
26. K. Zhang, W. Wang, S. Liu, X. Pan, J. Du, Y. Lou, S. Yu, S. Lv, N. Treps, C. Fabre, and J. Jing, "Reconfigurable hexapartite entanglement by spatially multiplexed four-wave mixing processes," Phys. Rev. Lett. **124**(9), 090501 (2020).
27. Z. Yan, L. Wu, X. Jia, Y. Liu, R. Deng, S. Li, H. Wang, C. Xie, and K. Peng, "Establishing and storing of deterministic quantum entanglement among three distant atomic ensembles," Nat. Commun. **8**(1), 718 (2017).
28. F. Hou, R. Quan, R. Dong, X. Xiang, B. Li, T. Liu, X. Yang, H. Li, L. You, Z. Wang, and S. Zhang, "Fiber-optic two-way quantum time transfer with frequency-entangled pulses," Phys. Rev. A **100**(2), 023849 (2019).
29. S. Lemieux, M. Manceau, P. R. Sharapova, O. V. Tikhonova, R. W. Boyd, G. Leuchs, and M. V. Chekhova, "Engineering the frequency spectrum of bright squeezed vacuum via group velocity dispersion in an SU(1, 1) interferometer," Phys. Rev. Lett. **117**(18), 183601 (2016).
30. X. Su, X. Jia, C. Xie, and K. Peng, "Generation of GHZ-like and cluster-like quadripartite entangled states for continuous variable using a set of quadrature squeezed states," Sci. China, Ser. G: Phys., Mech. Astron. **51**(1), 1–13 (2008).
31. P. van Loock and A. Furusawa, "Detecting genuine multipartite continuous-variable entanglement," Phys. Rev. A **67**(5), 052315 (2003).
32. T. Sh. Iskhakov, I. N. Agafonov, M. V. Chekhova, and G. Leuchs, "Polarization-entangled light pulses of 10^5 photons," Phys. Rev. Lett. **109**(15), 150502 (2012).
33. R. F. Dong, J. Heersink, J. Yoshikawa, O. Glöckl, U. Andersenand, and G. Leuchs, "An effcient source of continuous variable polarization entanglement," New J. Phys. **9**(11), 410 (2007).
34. K. Jensen, W. Wasilewski, H. Krauter, T. Fernholz, B. M. Nielsen, M. Owari, M. B. Plenio, A. Serafini, M. M. Wolf, and E. S. Polzik, "Quantum memory for entangled continuous-variable states," Nat. Phys. **7**(1), 13–16 (2011).
35. W. P. Bowen, N. Treps, R. Schnabel, and P. K. Lam, "Experimental demonstration of continuous variable polarization entanglement," Phys. Rev. Lett. **89**(25), 253601 (2002).
36. L. Wu, Z. Yan, Y. Liu, R. Deng, X. Jia, C. Xie, and K. Peng, "Experimental generation of tripartite polarization entangled states of bright optical beams," Appl. Phys. Lett. **108**(16), 161102 (2016).
37. N. Korolkova, G. Leuchs, R. Loudon, T. C. Ralph, and C. Silberhorn, "Polarization squeezing and continuous-variable polarization entanglement," Phys. Rev. A **65**(5), 052306 (2002).
38. V. Josse, A. Dantan, A. Bramati, M. Pinard, and E. Giacobino, "Continuous variable entanglement using cold atoms," Phys. Rev. Lett. **92**(12), 123601 (2004).
39. H. Yonezawa, T. Aoki, and A. Furusawa, "Demonstration of a quantum teleportation network for continuous variables," Nature **431**(7007), 430–433 (2004).
40. R. Ukai, N. Iwata, Y. Shimokawa, S. C. Armstrong, A. Politi, J. Yoshikawa, P. van Loock, and A. Furusawa, "Demonstration of unconditional one-way quantum computations for continuous variables," Phys. Rev. Lett. **106**(24), 240504 (2011).
41. X. Su, Y. Zhao, S. Hao, X. Jia, C. Xie, and K. Peng, "Experimental preparation of eight-partite cluster state for photonic qumodes," Opt. Lett. **37**(24), 5178 (2012).
42. L. Duan, G. Giedke, J. I. Cirac, and P. Zoller, "Inseparability criterion for continuous variable systems," Phys. Rev. Lett. **84**(12), 2722–2725 (2000).
43. Z. Yan and X. Jia, "Direct production of three-color polarization entanglement for continuous variable," J. Opt. Soc. Am. B **32**(10), 2139 (2015).